Prospecting polymetallic mineralization in Ardestan area, Central Iran, using fractal modeling and staged factor analysis

Akram Ostadhosseini[1], Mehrdad Barati*[2], Peyman Afzal[3], Insung Lee[4]

[1] *Department of Geology, University of Bu Ali Sina, Scientific Research Institute of Copper Gold Ardestan, Hamedan, Iran*

[2] *Department of Geology, University of Bu Ali Sina, Hamedan, Iran*

[3] *Department of Mining Engineering, South Tehran branch, Islamic Azad University, Tehran, Iran*

[4] *School of Earth and Environmental Sciences, Seoul National University, Seoul, South Korea*

**Corresponding author, e-mail: barati@basu.ac.ir*

(*received: 19/03/2018 ; accepted: 20/06/2018*)

Abstract

The purpose of this study is to determine geochemical anomalies on lithogeochemical data from Ardestan area, Central Iran, using concentration-number (C-N) fractal modeling and staged factor analysis. Staged factor analysis is used to the recognition of genetic correlation and elimination of non-indicator elements in three steps. Factor scores of elements were calculated and geochemical data classified by the C-N fractal model. According to the anomaly values, the distribution of elemental concentration for Mn and F1-3 were divided in four classes and five geochemical groups of Cu, Ag, Fe, F2-3 and F3-3 have been identified. Main geochemical anomalies are located in the NW, NE and SE of the study area. Obtained results from fractal and factor analyses is confirmed by field observations, petrographic and mineralographic studies, indicating pyrite, chalcopyrite, chalcocite, covellite, argentite, malachite, azurite, magnetite, hematite and pyrolusite are main ore minerals hosted by andesites and basaltic andesites.

Keywords*: Concentration–Number (C-N) Fractal Model, Staged Factor Analysis, Polymetallic Mineralization, Ardestan*

Introduction

Geochemical exploration methods are applied to mineral prospecting and identification of different types of deposits (Hawkes & Web, 1979; Carranza, 2009; Coker, 2010). Factor analysis is a multivariate analytical method in interpretation of the correlations between variables and variations in the multivariate datasets by a few factors. In factor analysis data is reduced into a few dimensions based on covariance or correlation matrix of variables and then a large number of variables are combined into a smaller set of variables or factors (Krumbein & Graybill, 1965; Tripathi, 1979; Johnson & Wichern, 2002; Zuo *et al*., 2013; Afzal *et al*., 2016; Parsa *et al*., 2016; Parsa *et al.,* 2018). This method is widely used to identify the intrinsic variability of a geochemical dataset and specify the geology and mineralization processes through the correlation between the geochemical data (Muller *et al.,* 2008; Yousefi *et al.,* 2012; Shamseddin Meigoony *et al.,* 2013; Afzal *et al.,* 2016). Yousefi *et al.* (2014) presented staged factor analytical method to remove non-indicator elements and identified significant geochemical signatures.

Specification of geochemical anomalies from a background is important in recognition and explanation of ore-forming processes (Hawkes & Webb, 1979; Kürzl, 1988; Cheng & Li, 2002; Carranza, 2008; Afzal *et al*., 2010; Hassanpour & Afzal, 2013; Zuo *et al.,* 2013; Nazarpour *et al.,* 2015; Chen & Cheng, 2016; Ghezelbash & Maghsoudi, 2018). For this purpose, several methods have been used, and the traditional methods are related to the frequency distribution of elements, including probability graphs, univariate and multivariate analyses (Hawkes & Webb, 1962; Rose *et al.,* 1979; Stanley & Sinclair, 1989; Gałuszka, 2007; Ziaii *et al.,* 2009). The main problem of these methods is that they do not remark the location and extent and magnitude of the anomaly, are unable to identify weak-intensity anomalies and do not provide spatial information of geochemical data (Cheng *et al.,* 1994; Afzal *et al.,* 2010). More recently, the spatial statistical methods such as fractal analysis and kriging consider factors such as spatial correlation and frequency distribution, correlation between adjacent samples, correlation coefficient, and reveal anomalies with low intensity that are hidden in a strong background (Grunsky & Agterberg, 1988; Cheng, 2007). The fractal modeling was established by Mandelbort (1983) which has been extensively utilized in geosciences, especially for determining the anomalous areas (Goncalves *et al.,* 2001; Lima *et al.,* 2003; Cheng & Agterberg, 2009; Sun *et al.,* 2009; Afzal *et al.,* 2010; Arias *et al.,* 2011; Wang *et al.,* 2011; Afzal *et al.,* 2013; Nazarpour *et al.,* 2015; Rezaei *et al.,* 2015; Wang & Zuo, 2015; Zhao *et al.,* 2015; Naimi-Ghassabian *et al.,* 2016; Afzal *et al.,* 2016; Chen *et al.,* 2016; Mohammadi *et al.,* 2016; Parsa *et al.,* 2016; Chen *et al.,* 2017; Parsa *et al.,* 2017a, b). First remarkable work in this field was carried out by Cheng *et al*. (1994) for the distinction of geochemical anomalies from background with concentration-area (C-A) and concentration-perimeter (C-P) methods on Mitchell-Sulphurets Cu-Au porphyry deposit in British Columbia, Canada. Based on these methods, developed techniques such as spectrum–area, concentrations–distance, simulated size–number, concentration–volume and singularity technique models were proposed (Cheng *et al.,* 1999; Li *et al.,* 2003; Zuo *et al.,* 2009; Cheng, 2012; Afzal *et al.,* 2011; 2015; 2017; Sadeghi *et al.,* 2012; 2015; Feizi *et al.,* 2017). These methods are applied to the determination of geochemical anomalies and mineralization zones in geochemical exploration, economic geology and geophysics. On this point, the C-N fractal modeling and staged factor analysis are used to identify geochemical signatures and specification of geochemical anomalies in this study.

Finally, obtained results were validated by lithogeochemical data, petrography, mineralography, alterations and field observations.

Geological setting

The study area is located 21 km to the SW of Ardestān city and 80 km to the NE of Esfahan (Central Iran). This area is situated in the central part of Sahand-Bazman (Uriumieh-Dokhtar) Magmatic Belt (SBMB) based on the sedimentary-structural divisions (Fig. 1; Aghanabati, 2006). The SBMB is extended parallel to Zagros thrust and Sanandaj-Sirjan structural zones. Volcanic activity in this belt started from Cretaceous and has been continued Quaternary. This magmatic assemblage includes volcanic rocks with a range of basic to acidic, tuff, agglomerate and plutonic rocks. The SBMB results from Neotethyan oceanic subduction beneath Central Iran plate from Mesozoic to Cenozoic (Stocklin, 1977; Berberian & King, 1981; Alavi, 1994; Shahabpour, 2005; Allen *et al.,* 2006; Ghasemi & Talbot, 2006). This magmatic belt represents geochemical characteristics of subduction zones with features of calc-alkaline to alkaline magma affinity (Berberian & King, 1981; Shahabpour, 2007; Omrani *et al.,* 2008; Dargahi *et al.,* 2010; Rajabpour *et al.,* 2017). The SBMB is important from the aspect of structural geology and tectonics because of large active faults, including Qom-Zefreh fault and its situation among geological provinces of Central Iran, Sanandaj-Sirjan and Zagros folded belt. The SBMB hosts porphyry Cu±Mo±Au deposits such as Sungun, Sarcheshmeh, Meiduk, Kahang and Darehzar (Dewey *et al.,* 1973; Brookfield, 1977; Farhoudi, 1978; Shahabpour, 1994; Atapour & Aftabi, 2007; Boomeri *et al.,* 2009; Daneshvar Saein, 2012; Zarasvandi *et al.,* 2015; Jamali, 2017; Rajabpour et al., 2017) and other associated deposits with this geodynamic origins such as copper-gold porphyry, gold epithermal and manganese-iron (Bazin & Hubner, 1969; Amidi & Emami, 1984; Shahabpour, 1994; Shafiei *et al.,* 2009).

Different stages of Cenozoic magmatic activity in the middle segment of the SBMB around the Ardestān area consists of different successions of volcanic and intrusive rocks (Fig. 1). The Miocene diorite- monzodiorite bodies intruded into the Eocene volcanic units. In the southwest of the area, these intrusive units are juxtaposed with a fault boundary (Marbin reverse fault) adjacent to Eocene volcanic units. Eocene volcanic units include basaltic andesite, andesite, rhyodacite, rhyolite, tuffs and ignimbrites. Alteration zones, developed in rock types, include propylitic, argillic, siliceous and carbonateous. The Cu ore mineral occurrences are numerous and consist mostly of malachite and azurite within calcite and quartz veins. Sulfide minerals consist of pyrite, chalcopyrite, argentite, chalcocite, bornite, covellite and oxide minerals are magnetite, hematite, goethite and pyrolusite. There are three major structural features with trends of the N–S, NW-SE and NE–SW faults (Fig. 1).

Methodology

Staged factor analysis

The staged factor analysis is a multivariate analytical method that reduces the number of geochemical variables to a few and creates some correlations among these variables (Carranza & Hale, 1997; Cheng, 2010). The staged factor analysis, categorizes geochemical data and determines indicator elements related to target deposit (Johnson & Wichern, 2002; Yousefi et al., 2014; Wang & Zuo, 2015). In this method, the combination of variables, instead of one single variable, are applied; therefore, increases the possibility detection of geochemical halo around the ore body and identifies anomalies associated with mineralization, and decreases the effects of random errors in using of combined variables (Yousefi *et al.,* 2012). The maximum likelihood method (ML) and principal factor analysis (PFA), which operates basically like principal component analysis (PCA) but with a decreased correlation or covariance matrix, are used to extract the prevalent factors in factor analysis (Reimann *et al.,* 2002; Treiblmaier & Filzmoser, 2010).The principal component analysis was applied to extract factors in this study. Varimax rotation function utilized and factors with eigenvalues greater than 1 were remained (Kaiser, 1958). Finally, the elements with threshold values of 0.6 and higher were considered.

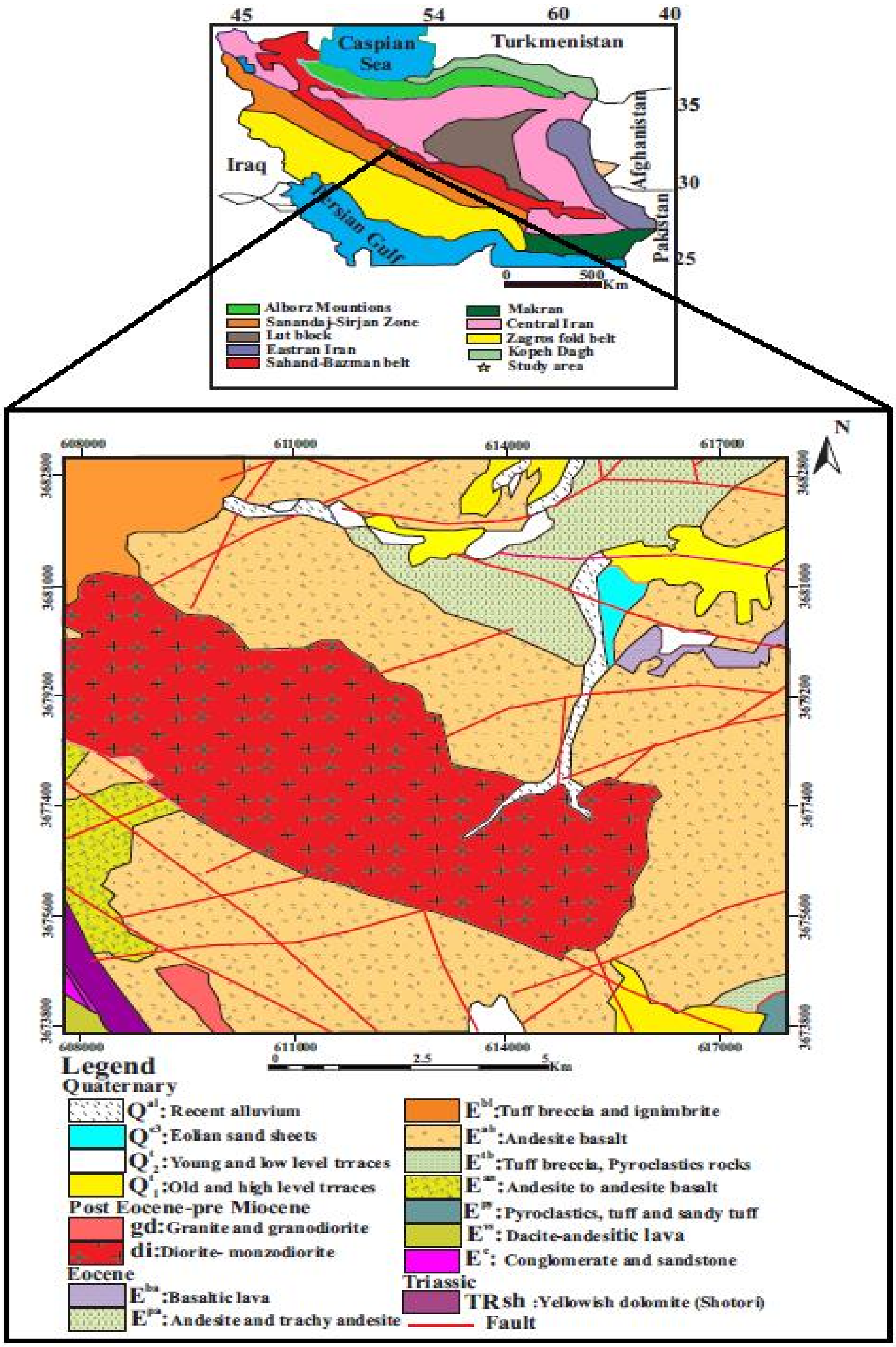

Figure 1. Location of Ardestan in the structural map of Iran (Stocklin, 1977) and geological map of the study area (Radfar, 1999).

C-N fractal modeling

The C–N fractal model was established for defining anomaly values. The C-N fractal model is based on an inverse relationship between elemental concentration and cumulative frequency of samples (Wang *et al.,* 2008; Zuo *et al.,* 2009; Hassanpour & Afzal, 2013; Rezaei *et al.,* 2015). This model is presented by the following equation:

$$N(\geq C) \propto \rho^{-\beta}. \quad (1)$$

Where N (≥C) indicate the number of samples that have concentration values higher or equal to ρ value. The ρ is elemental concentration and β is the fractal dimension. An important advantage of this model is that calculations can be performed before estimating raw data and the raw data may not have been undergone pre-treatment and evaluation (Deng *et al*., 2010; Hassanpour & Afzal, 2013).

Discussion and results

In this study, 90 lithogeochemical samples were collected from the deposit, and analyzed by inductively coupled plasma mass spectrometry (ICP–MS) method at the Zarazma company in Iran for 56 elements. Pb, Ag, Mn, Fe,Co, Ni,V, Zn and Cu are the exploration target. Detection limits are 0.1 ppm, 5 ppm and 100 ppm for Ag, Mn and Fe, respectively and 1 ppm for Co, Ni,V, Zn, Pb and Cu. Staged factor analysis, used to determine significant geochemical signatures and elements, was classified using factor analysis by the SPSS software package. For this purpose, three steps of factor analysis were performed on geochemical data for recognizing significant multi element associations (Table 1).

In the first stage, the elements with values less than 0.6 including Mg, W and Cr were removed. The second stage of factor analysis was performed on the remaining data other than Ba, Ca, P, U, Ti, Mo, As and Sn.

Table1 Rotated factor matrix for three stages of staged factor analysis.

Element	First stage					
	1	2	3	4	5	6
Ag	0.191	0.247	0.892	-.064	0.133	0.004
Ba	-.069	-.188	-.022	0.321	-.603	0.011
Ca	0.164	-.252	0.046	0.044	0.745	0.351
Cu	0.242	0.258	0.828	.170	-.154	0.068
Fe	0.612	-.099	0.057	0.642	0.228	-.015
Mg	0.340	-.244	0.524	0.430	0.108	0.321
Mo	-.196	0.657	0.221	0.324	0.216	-.237
Mn	0.884	-.168	0.237	-.044	0.170	0.049
P	-.153	0.086	-.029	0.031	0.186	0.819
Pb	0.644	0.045	0.021	0.105	-.162	0.273
Sn	-.032	0.906	0.110	-.169	0.070	-.084
W	0.159	0.529	0.059	0.591	-.385	0.038
V	0.226	-.096	0.103	0.821	-.117	0.234
U	-.071	0.919	0.100	-.110	-.101	0.063
Ti	0.197	-.423	0.162	0.233	0.097	0.766
Zn	0.802	-.087	0.333	0.255	-.146	0.063
Ni	0.755	-.025	0.276	0.181	0.415	-.239
Co	0.910	-.011	-.033	0.079	0.159	-.179
Cr	-.044	-.116	0.511	0.490	0.391	-.334
As	0.047	0.035	0.011	0.086	0.743	0.066

Element	Second stage					
	1	2	3	4	5	6
Ag	0.189	0.225	0.185	0.897	0.005	-.009
Ba	0.010	-.121	-.701	-.088	0.205	0.130
Ca	0.141	-.243	0.764	0.014	0.144	0.328
Cu	0.215	0.185	-.093	0.894	0.186	0.028
Fe	0.595	-.065	0.170	0.038	0.720	-.002
Mo	-.128	0.772	0.097	0.139	0.336	-.122
Mn	0.888	-.171	0.178	0.208	0.012	0.053
P	-.118	0.106	0.131	-.058	0.006	0.882
Pb	0.657	0.011	-.198	0.051	0.054	0.317
Sn	0.1	0.906	0.049	0.119	-.231	-.057
V	0.162	-.119	-.134	0.157	0.872	0.167
U	-.071	0.876	-.100	0.174	-.167	0.054
Ti	0.194	-.432	0.089	0.134	0.239	0.761
Zn	0.817	-.133	-.139	0.327	0.174	0.075
Ni	0.781	0.028	0.384	0.189	0.231	-.209
Co	0.908	-.004	0.145	-.052	0.118	-.176
As	0.076	0.040	0.741	-.025	0.047	0.107

Element	Third stage			
	1	2	3	4
Ag	0.165	0.942	0.080	-.066
Cu	0.141	0.922	0.030	0.237
Fe	0.720	0.061	-.071	0.611
Mn	0.033	0.038	0.900	-.044
Pb	0.213	0.073	0.834	0.217
V	0.115	0.105	0.148	0.955
Zn	0.679	0.323	0.266	0.290
Ni	0.908	0.250	0.068	0.046
Co	0.956	0.004	0.153	0.032

Furthermore, the third step has obtained four factors with threshold values greater than 0.6 including Fe, Co, Ni, Zn (factor1), Cu and Ag (factor2), Mn, Pb (factor3) and V (factor4). Regarding the type of mineralization, three factors (F1-3, F2-3 and F3-3) were considered.

After using staged factor analysis to identify geochemical signatures, the C-N method was utilized for determination of anomaly values on resulted factors and raw data that indicated a multifractal nature in the study area (Figs. 2 and 3). Log-log plots were generated and break points separated by stright lines, were considered as different geochemical populations. Based on C-N log-log plots, four geochemical populations were specified for F1-3, Mn and five geochemical populations were identified for F2-3, F3-3, Cu, Ag and Fe. Strong anomaly for Cu, Ag, Fe and Mn based on the C-N fractal modeling starting from 19952 ppm, 177 ppm, 63098 ppm and 6607ppm, respectively, as depicted in table 2.

Table 2 Anomaly values of Cu, Ag, Fe and Mn based on the C-N fractal model in the Ardestan area.

Element (ppm)	High background	Weak anomaly	Strong anomaly	Very strong anomaly
Cu	562	1000	7079	19952
Ag	0.63	3.16	6.3	177
Fe	28184	38019	50119	63098
Mn	631	4169	6607	-

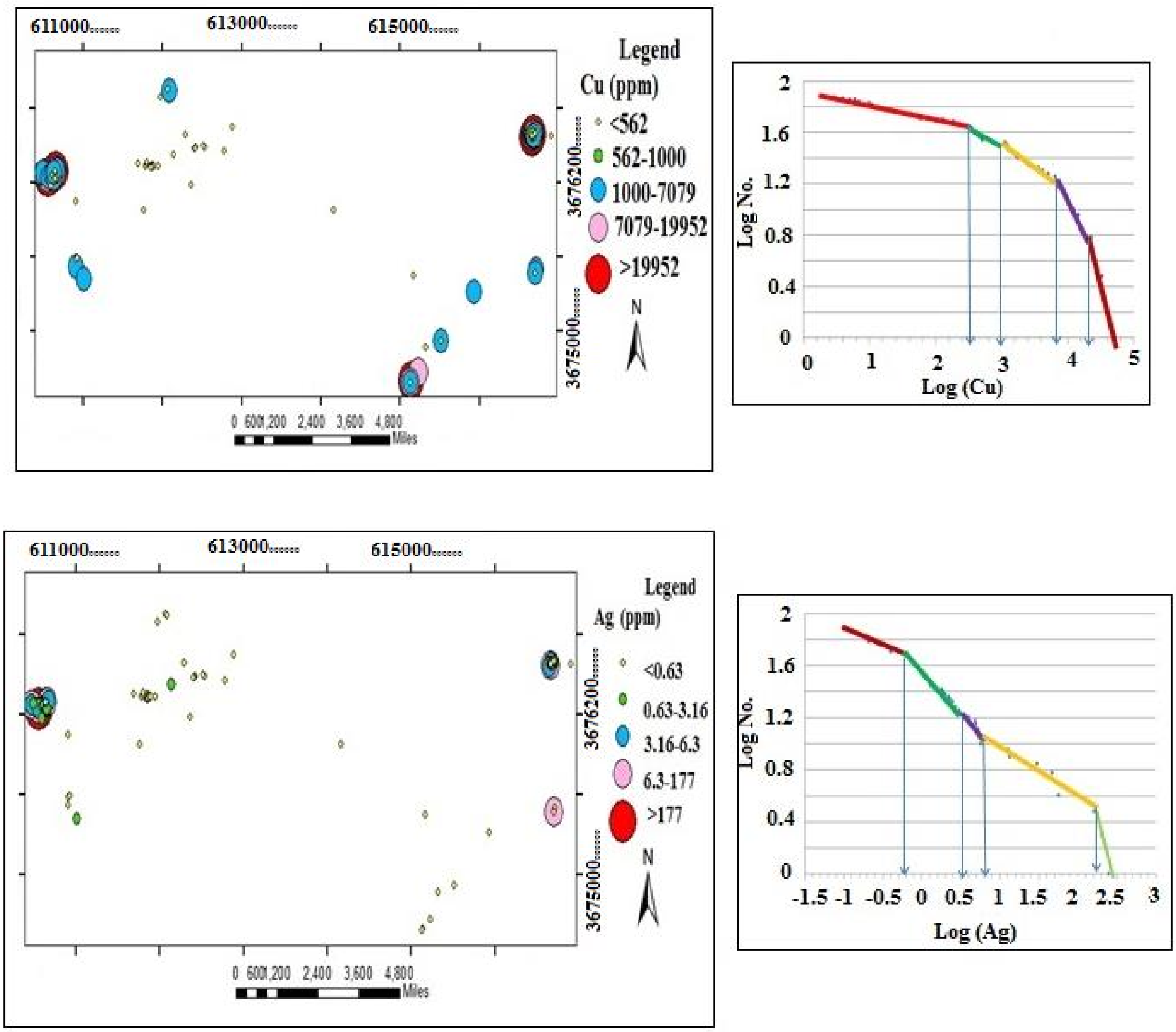

Figure 2. Log-log plots and geochemical maps derived from C-N fractal model of Cu, Ag, Mn and Fe in the study

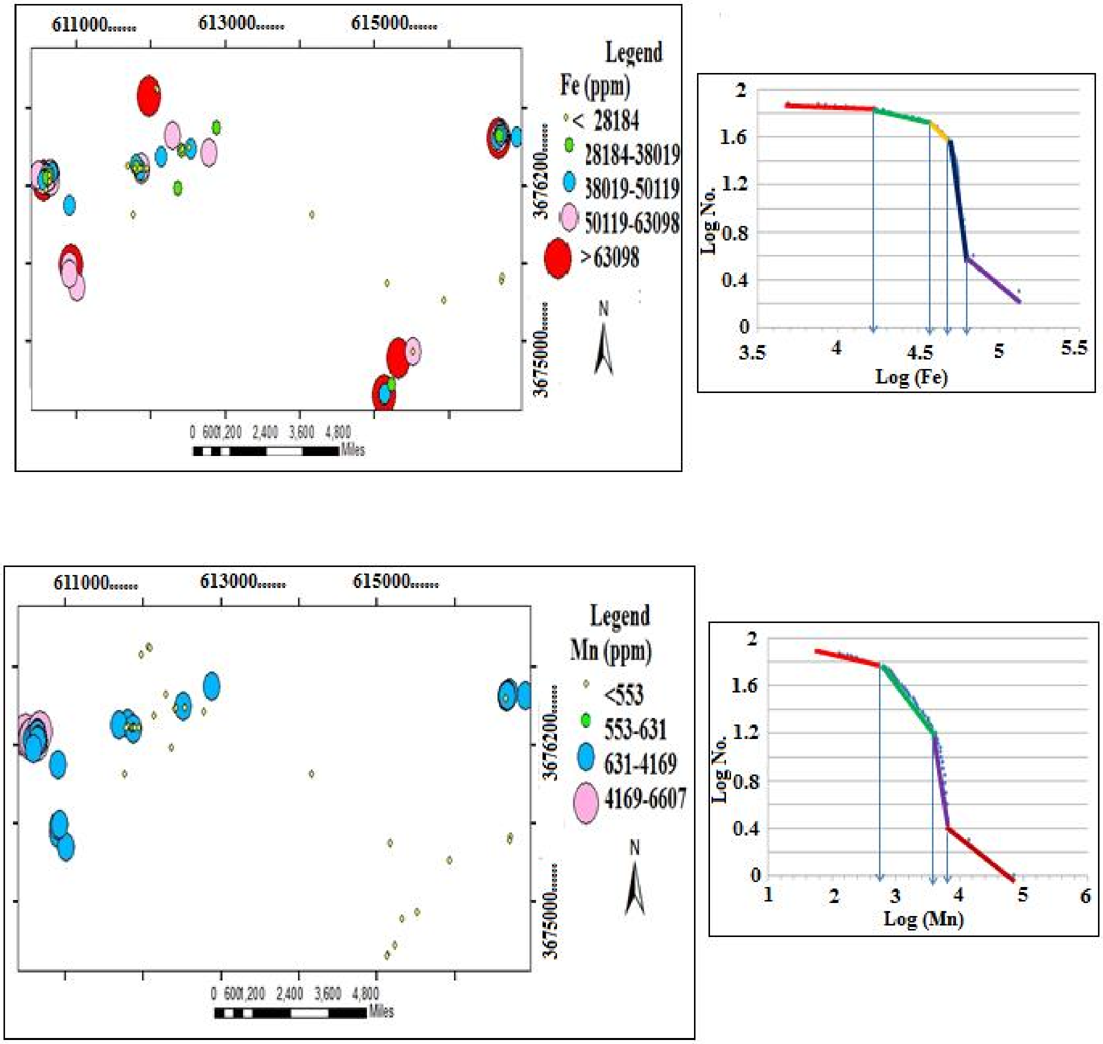

area.

Figure 2. To be continued

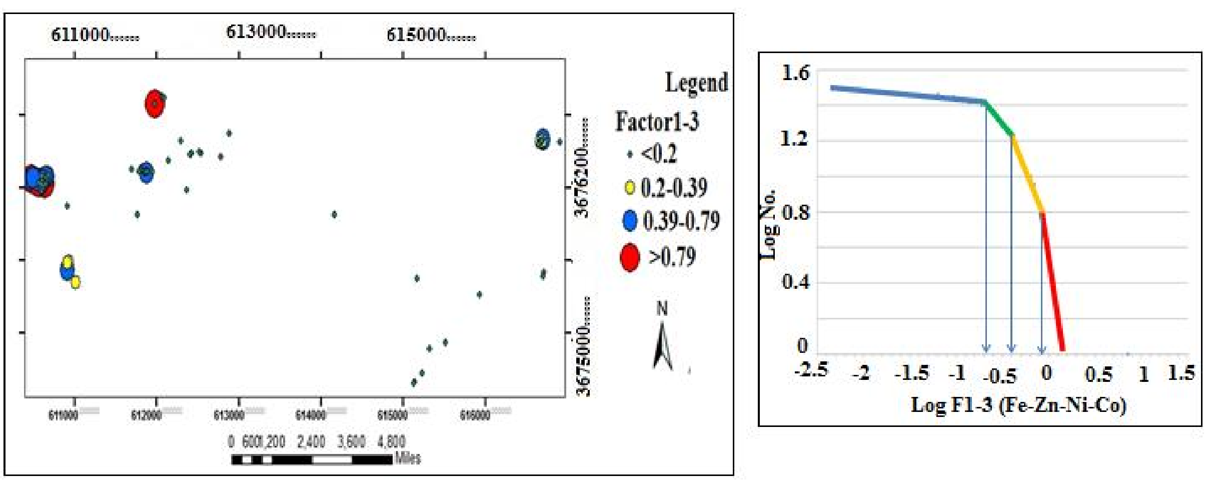

Figure 3. Log-log plots and geochemical maps obtained from C-N fractal model for F1-3, F2-3 and F3-3 in the study area.

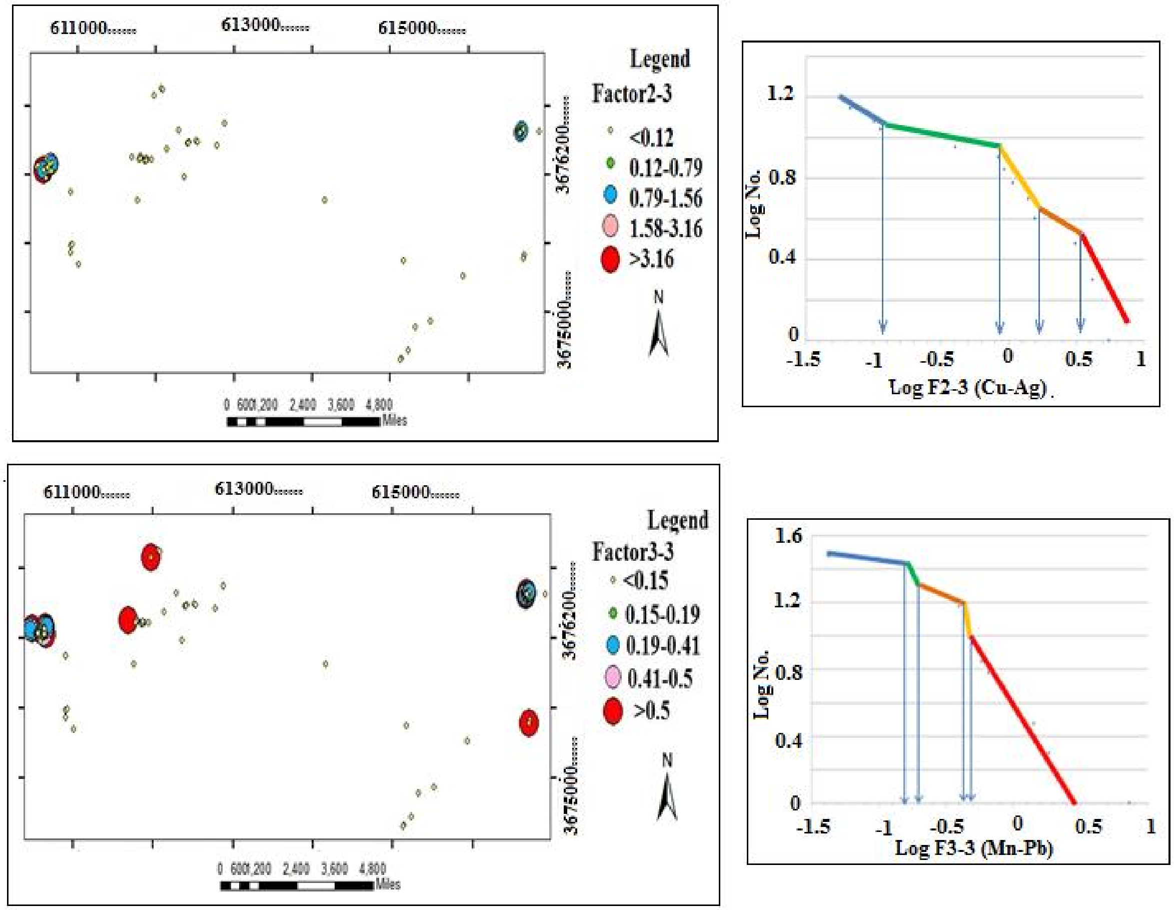

Figure 3. To be continued

The geochemical maps were constructed using ArcGIS software (Fig. 2). Based on the generated symbol maps, most of the Cu anomalies are situated in the SE, NE and NW parts of the study area in the basaltic andesite, trachyandesite and andesite rocks (Fig. 2). Strong anomaly of Ag are located in the NW and NE parts of this area in the andesites and andesitic basalts, as indicated in Fig. 2.

Strong anomaly of Fe are observed in the SE, NE, NW and western parts of the study area in the basaltic andesites and andesites. Moreover, Mn anomalies appeare in the NW of the area in andesites (Fig. 2).

Strong anomaly for F1-3, F2-3 and F3-3 are situated in the NW and NE parts, NW part and NW, NE, SE of the study area (Fig. 3), respectively, where factor analysis maps show appropriate correlation with elemental geochemical maps.

Field observation

The promising metal-bearing regions derived by data processing were validated with field study and sampling. Field observation and petrographic studies indicate the study area is mainly composed of volcanic rocks including basaltic andesite, basalt, andesite, trachy andesite, rhyolite, rhyodacite, tuff, ignimbrite, and also intrusive rocks including diorite, monzodiorite and granodiorite (Figs. 4a and 5). The dominant textures of these rocks are microlithic porphyry, granular and glomeroporphyritic (Fig. 5).

The hydrothermal activities had affected volcanic, subvolcanic and intrusive rocks and created a variety of alteration in this area. Propilitic, silicic, carbonaceous, argillic and sercitic alterations are recognized in these rocks. Propylitic alteration is extensive and is observed in most locations. Sericite, epidote, chlorite, hematite, iddingsite and calcite are the most important minerals produced by alteration (Fig. 5). Iddingsite ($MgFe_2Si_3O_{10}$-4(H_2O)), common product of mafic minerals, is chemically formed by entering iron and water into mafic minerals (Shelley, 1993).

Figure 4. Field photographs from the study area. (a) Views of rock units where diorite units penetrate into the andesitic basalt units (looking NE); (b) Iron and manganese mineralization in andesitic basalts (looking NE); (c) The presence of malachite and azurite in the andesite.

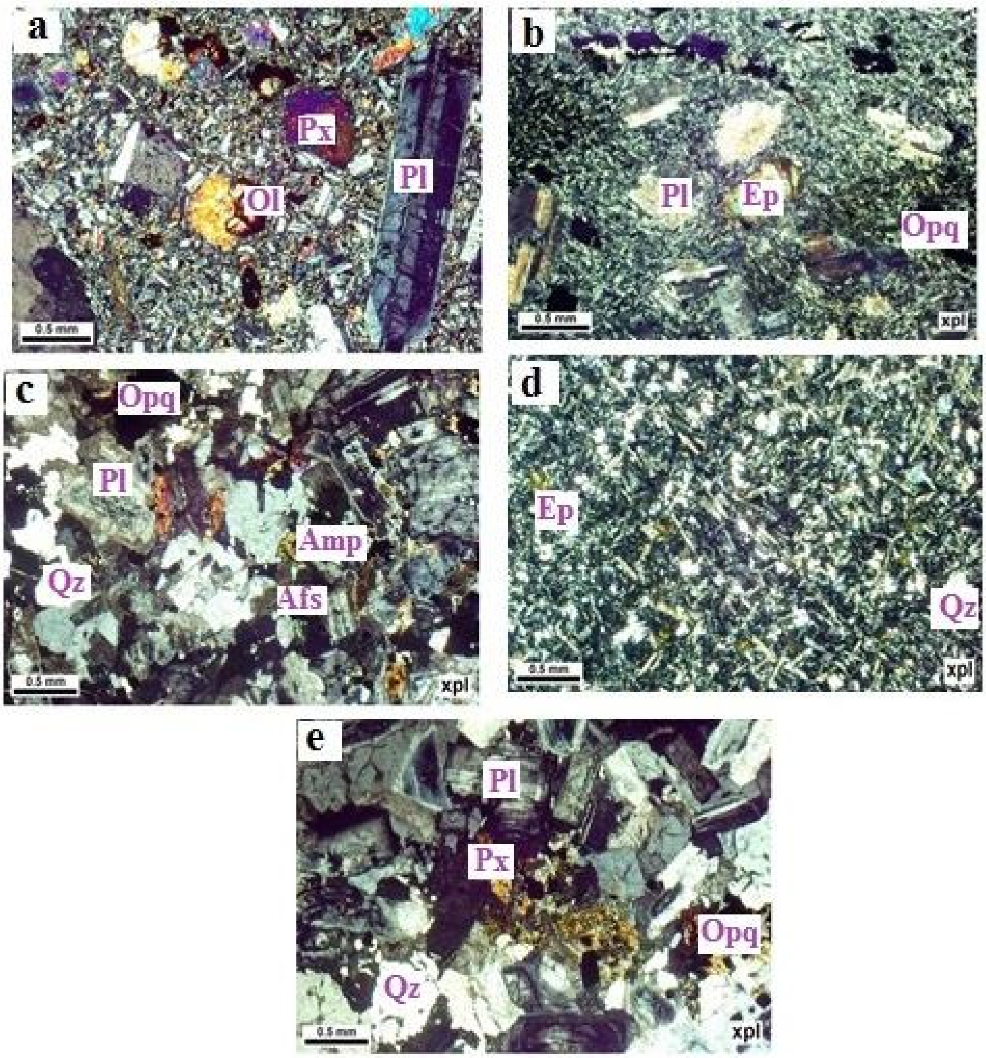

Figure 5. Photomicrographs of mineral assemblages and textural features of the studied rocks. (a) Plagioclase and pyroxene phenocrysts in basalts and olivine subhedral crystals which are replaced by iddingsite (XPL); (b) Trachyandesite with porphyritic texture (XPL); (c) The presence of plagioclase, amphibole and K-feldspars with granular texture in the granodiorite rock (XPL); (d) Alteration of minerals in rhyodacite to epidote (XPL); (e) Pyroxene in diorite that is replaced by chlorite (XPL) (Pl= Plagioclase; Px= Pyroxene; Amp= Amphibole; Ep= epidote; Qz= Quartz; Opq= opaque; Afs= Potassium feldspar; Ol= Olivine).

The principal gangue minerals are barite, chlorite, epidote with lesser amounts of quartz and calcite. The obtained results from mineralographic studies indicate mineralization occurs in volcanic and subvolcanic rocks and presents the two phases of mineralization in this area, sulfide minerals consisting of pyrite, chalcopyrite, argentite, chalcocite, bornite, covellite and, oxide minerals including magnetite, hematite, goethite, pyrolusite that usually exist with silica, calcite and barite vein-veinlet (Fig. 6). Styles of mineralization are massive, veins, disseminated and stockwork in this area, as depicted in Fig. 6.

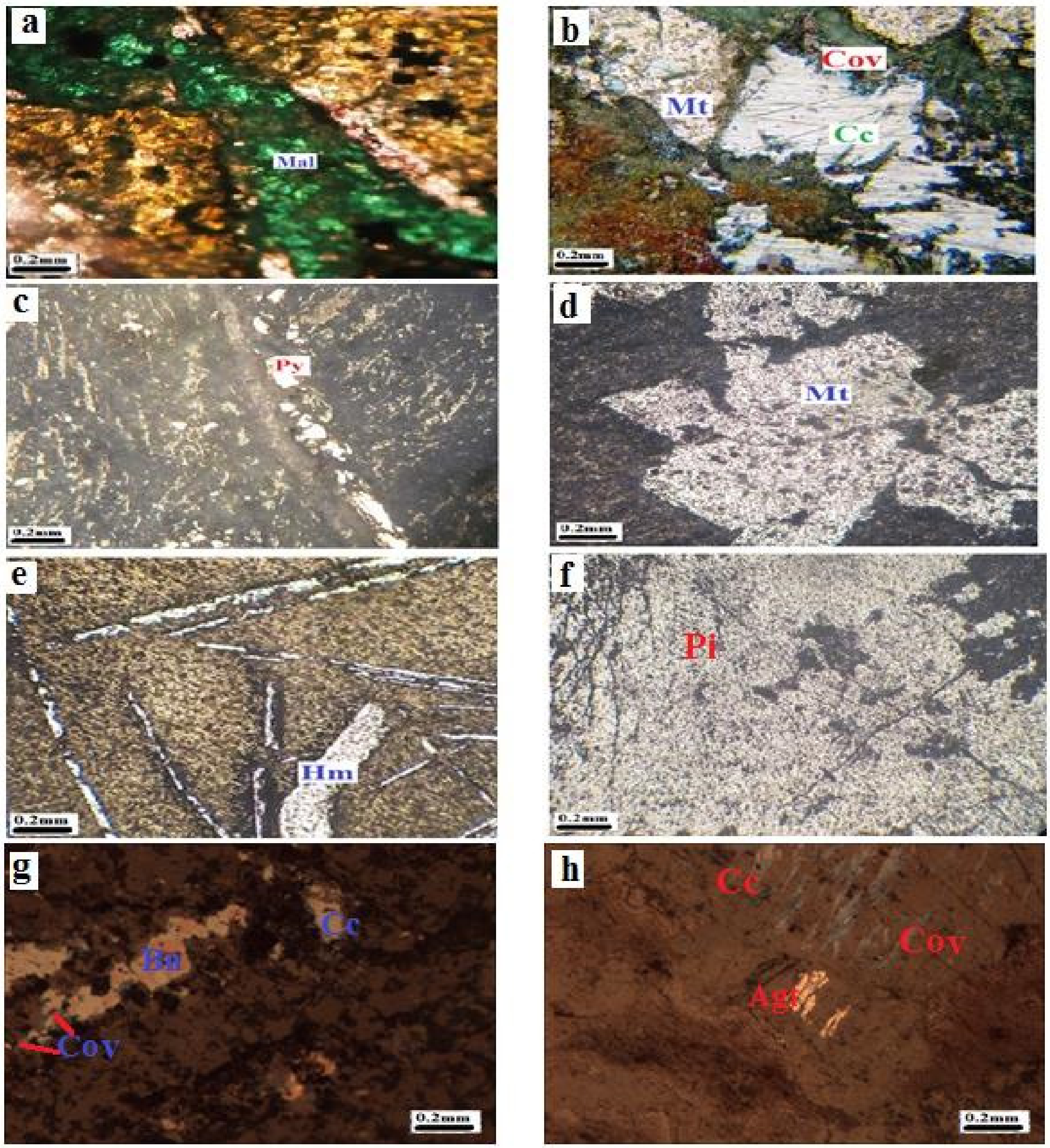

Figure 6. Photomicrographs of the ore minerals in the study area. (a) Malachite with vein texture (reflected light); (b) Chalcocite replaced by covellite (reflected light); (c) Pyrite with disseminated and vein texture (reflected light); (d) Massive magnetite (reflected light); (e) Bladed crystals of hematite (reflected light); (f) Pyrolusite with fine-grained and massive texture (reflected light); (g) Bornite, chalcocite and covellite in andesite; (h) Argentite, chalcocite and covellite (Mal, Malachite; Mt, Magnetite; Py, Pyrite; Cc, Chalcocite; Cov, Covellite; Hm, Hematite; Pi, Pyrolusite; Bn, Bornite; Agt, Argentite).

Iron oxides occur as magnetite and hematite in andesite and basaltic andesite with two outcrops in the SE and NW of the Ardestan area (Fig. 4b), also numerous andesite dikes with iron mineralization as hematite and goethite are observed in the western part of the study area (Fig. 7). Copper minerals mostly are observed as copper carbonates (malachite and azurite) in the andesites, trachy andesites and basaltic andesite in the NE, SE and NW part of the study area (Fig. 4c).

Figure 7. The image of andesite dikes with iron mineralization in the west of the study area.

Conclusion

In this study, the staged factor and the C-N fractal analysis are applied to identify geochemical anomalies. Using staged factor analysis, geochemical data was categorized and indicator elements related to mineralization were determined. For this purpose, three steps of factor analysis were performed on geochemical data and based on the type of mineralization and exploration target, three factors (F1-3, F2-3 and F3-3) were extracted. The C-N model was carried out for the determination of anomaly values on cleaning factors and raw data. Based on the C-N log-log plots, four geochemical populations were specified for F1-3, Mn and five geochemical populations for F2-3, F3-3, Cu, Ag and Fe. Strong anomaly for Cu, Ag, Fe and Mn based on the C-N fractal model commence from 19952 ppm, 177 ppm, 63098 ppm and 6607 ppm, respectively. Most of the high-intensity elemental anomalies are situated in the SE, NE and NW parts of the study area. The enrichment of Cu, Fe, Ag and Mn are correlated with the volcanic units of the basaltic andesite and andesite. Results obtained from factor analysis indicate appropriate correlation with elemental distribution maps. Geological evidence including field observations, petrographic, mineralographic and alteration studies confirm the obtained results of these methods. Therefore, these methods can be considered as effective methods for geochemical anomaly separation and to determine the promising regions in the study area.

Acknowledgements

The present study was supported by the Cu-Au company of ardestan. The authors are grateful to Mr. Sharif for providing sampling facilities and let us access to drill cores and exploration data.

References

Afzal, P., Eskandarnejad Tehrani, M., Ghaderi, M., Hosseini, M.R., 2016. Delineation of supergene enrichment, hypogene and oxidation zones utilizing staged factor analysis and fractal modeling in Takht-e-Gonbad porphyry deposit, SE Iran. Journal of Geochemical Exploration, 161: 119-127.

Afzal, P., Ahmadi, K., Rahbar, K., 2017. Application of fractal-wavelet analysis for separation of geochemical anomalies. Journal of African Earth Sciences, 128: 27-36.

Afzal, P., Aramesh Asl, R., Adib, A., 2015. Application of fractal modeling for Cu mineralization reconnaissance by ASTER multispectral and stream sediment data in Khoshname area, NW Iran. Journal of the Indian Society of Remote Sensing, 43: 121–132.

Afzal, P., Fadakar Alghalandis, Y., Khakzad, A., Moarefvand, P., RashidnejadOmran, N., 2011. Delineation of mineralization zones in porphyry Cu deposits by fractal concentration–volume modeling. Journal of Geochemical Exploration, 108: 220–232.

Afzal, P., Harati, H., Fadakar Alghalandis, Y., Yasrebi, A.B., 2013. Application of spectrum–area fractal model to identify of geochemical anomalies based on soil data in Kahang porphyry-type Cu deposit, Iran. Chemie der Erde-Geochemistry, 73: 533–543.

Afzal, P., Khakzad, A., Moarefvand, P., Rashidnejad, N., Esfandiari, B., Alghalandis,Y.F., 2010. Geochemical anomaly separation by multifractal modeling in Kahang porphyry system, Central Iran, Journal of Geochemical Exploration, 104: 34–46.

Aghanabati, A., 2006. Geology of Iran. Geological Survey of Iran, Tehran, 586p. (in Persian).

Alavi, M., 1994. Tectonics of zagros orogenic belt of Iran, new data and interpretation. Tectonophysics, 229: 211–238.

Allen, M.B., Blanc, E.J.P., Walker, R., Jackson, J., Talebian, M., Ghassemi, M.R., 2006. Contrasting styles of convergence in the Arabia–Eurasia collision: why escape tectonics does not occur in Iran. Geological Society of America, Special Paper, 409p.

Amidi, S. M., Emami, M. H., Michel, R., 1984. Alkaline character of Eocene volcanism in the middle part of Central Iran and its geodynamic situation. Geologische Rundschau, 73: 917-932.

Arias, M., Gumiel, P., Sanderson, D.J., Martin-Izard, A., 2011. A multifractal simulation model for the distribution of VMS deposits in the Spanish segment of the Iberian Pyrite Belt. Computers & Geosciences, 37: 1917-1927.

Atapour, H., Aftabi, A., 2007. The geochemistry of gossans associated with Sarcheshmeh porphyry copper deposit, Rafsanjan, Kerman, Iran: Implications for exploration and the environment. Journal of Geochemical Exploration, 93: 47-65.

Bazin, D., Hübner, H., 1969. Copper deposits in Iran: Iran Geological Survey, Tehran, 232 p.

Berberian, M., King, G.C.P., 1981. Towards a paleogeography and tectonic evolution of Iran. Canadian Journal of Earth Sciences, 18: 210-265.

Boomeri, M., Nakashima, K., Lentz, D.R., 2009. The Miduk porphyry Cu deposit, Kerman, Iran: A geochemical analysis of the potassic zone including halogen element systematics related to Cu mineralization processes. Journal of Geochemical Exploration, 103: 17-19.

Brookfield, M.E., 1977. The emplacement of giant ophiolite nappes: I. Mesozoic-Cenozoic examples. Tectonophysics, 37: 247-303.

Carranza, E.J.M., Hale, M., 1997. A catchment basin approach to the analysis of eochemical-geological data from Albay province, Philippines. Journal of Geochemical Exploration, 60: 157–171.

Carranza, E.J.M., 2008. Geochemical anomaly and mineral prospectivity mapping in GIS. Handbook of Exploration and Environmental Geochemistry, 11: 1–351

Carranza, E.J.M., 2009. Controls on mineral deposit occurrence inferred from analysis of their spatial pattern and spatial association with geological features. Ore Geology Reviews, 35: 383-400.

Chen, G., Cheng, Q., 2016. Singularity analysis based on wavelet transform of fractal measures for identifying geochemical anomaly in mineral exploration. Computers and Geosciences, 87: 56-66.

Chen, Z., Chen, J., Tian, S., Xu, B., 2017. Application of fractal content-gradient method for delineating geochemical anomalies associated with copper occurrences in the Yangla ore field, China. Geoscience Frontiers, 8: 189-197.

Cheng, Q., Xia, Q., Li, W., Zhang, S., Chen, Z., Zuo, R., Wang, W., 2010. Density/area power – law models for separating multi-scale anomalies of ore and toxic elements in stream sediments in Gejiu mineral district, Yunnan Province, China. Biogeosciences, 7: 3019–3025.

Cheng, Q., 2007. Multifractal imaging filtering and decomposition methods in space, Fourier frequency and eigen domains. Nonlinear Processes in Geophysics, 14: 293–303.

Cheng, Q., 2012. Singularity theory and methods for mapping geochemical anomalies caused by buried sources and for predicting undiscovered mineral deposits in covered areas. Journal of Geochemical Exploration, 122: 55–70.

Cheng, Q., Agterberg, F.P., 2009. Singularity analysis of ore-mineral and toxic trace elements in stream sediments. Computers and Geosciences, 35: 234-244.

Cheng, Q., Agterberg, F.P., Ballantyne, S.B., 1994. The separation of eochemical anomalies from background by fractal methods. Journal of Geochemical Exploration, 51: 109–130.

Cheng, Q., Xu, Y., Grunsky, E., 1999. Integrated spatial and spectral analysis for geochemical anomaly separation. Natural Resources Research, 9: 43-51.

Cheng, Q., Li, Q., 2002. A fractal concentration-area method for assigning a color palette for image representation. Computers Geoscience, 28: 567-575.

Coker, W.B., 2010. Future research directions in exploration geochemistry. Geochemistry Exploration Environment Analysis, 10: 75–80.

Daneshvar Saein, L., Rasa, I., Rashidnejad Omran, N., Moarefvand, P., Afzal, P., 2012. Application of concentration-volume fractal method in induced polarization and resistivity data interpretation for Cu-Mo porphyry deposits exploration, case study: Nowchun Cu-Mo deposit, SE Iran. Nonlinear Processes in Geophysics, 19: 431-438.

Dargahi, S., Arvin, M., Pan, Y., Babaei, A., 2010. Petrogenesis of post-collisional A-type granitoid from the Urumieh-Dokhtar magmatic assemblage, Southwestern Kerman Iran, Constraints on the Arabian-Eurasian continental collision. Lithos, 115: 190–204.

Deng, J., Wang, Q., Yang, L., Wang, Y., Gong, Q., Liu, H., 2010. Delineation and explanation of geochemical anomalies using fractal models in the Heqing area, Yunnan Province, China. Journal of Geochemical Exploration, 105: 95–105.

Dewey, J.F., Pitman, W.C., Ryan, W.B., Bonnin, J., 1973. Plate tectonic and evolution of the Alpine system. Geological Society of America Bulletin, 84: 3137–3180.

Farhoudi, G.A., 1978. Comparison of Zagros geology to island arcs. The Journal of Geology, 86: 323–334.

Feizi, F., Karbalaei Ramzanali, A., Mansouri, E., 2017. Calcic iron skarn prospectivity mapping based on fuzzy AHP method, a case Study in Varan area, Markazi province, Iran. Geosciences Journal, 21: 123-136.

Gałuszka, A., 2007. A review of geochemical background concepts and an example using data from Poland. Environmental Geology, 52: 861–870.

Ghasemi, A., Talbot, C.J., 2006. A new tectonic scenario for the Sanandaj–Sirjan Zone (Iran). Journal of Asian Earth Sciences, 26: 683–693.

Ghezelbash, R., Maghsoudi, A., 2018. Comparison of U-spatial statistics and C-A fractal models for delineating anomaly patterns of porphyry-type Cu geochemical signatures in the Varzaghan district, NW Iran. Comptes Rendus Geoscience. DOI: 10.1016/j.crte.2018.02.00

Gonçalves, M.A., Mateus, A., Oliveira, V., 2001. Geochemical anomaly separation by multifractal modeling. Journal of Geochemical Exploration, 72: 91-114.

Grunsky, E.C., Agterberg, F.P., 1988. Spatial and multivariate analysis of geochemical data from metavolcanic rocks in the Ben Nevis Area, Ontario. Mathematical Geology, 20: 825-861.

Hassanpour, S., Afzal, P., 2013. Application of concentration–number (C–N) multifractal modeling for geochemical anomaly separation in Haftcheshmeh porphyry system, NW Iran. Arabian Journal of Geosciences, 6: 957–970.

Hawkes, H.E., Webb, J.S., 1962. Geochemistry in mineral exploration. Harper and Row, New York, 415 p.

Hawkes, H.E., Webb, J.S., 1979. Geochemistry in mineral exploration, 2nd edn. Academic Press, New York, 657 p.

Jamali, H., 2017. The behavior of rare-earth elements, zirconium and hafnium during magma evolution and their application in determining mineralized magmatic suites in subduction zones: Constraints from the Cenozoic belts of Iran. Ore Geology Reviews, 81: 270–279.

Johnson, R.A., Wichern, D.W., 2002. Applied Multivariate Statistical Analysis, 5th edn. Prentice Hall, New Jersey, 773p.

Kaiser, H.F., 1958. The varimax criteria for analytical rotation in factor analysis. Psychometrika, 23: 187–200.

Krumbein, W.C., Graybill, F.A., 1965. An Introduction to Statistical Models in Geology. McGraw-Hill, New York, 457p.

Kürzl, H., 1988. Exploratory data analysis: recent advances for the interpretation of geochemical data. Journal of Geochemical Exploration, 30: 309-322.

Li, C., Ma, T., Shi, J., 2003. Application of a fractal method relating concentrations and distances for separation of geochemical anomalies from background. Journal of Geochemical Exploration, 77: 167–175.

Lima, A., De Vivo, B., Cicchella, D., Cortini, M., Albanese, S., 2003. Multifractal IDWinterpolation and fractal filtering method in environmental studies: an application on regional stream sediments of (Italy), Campania region. Applied Geochemistry, 18: 1853–1865.

Mandelbrot, B.B., 1983. The Fractal Geometry of Nature, Updated and Augmented Edition. Freeman, New York, 468 p.

Mohammadi, N.m., Hezarkhani, A., Shokouh Saljooghi, B., 2016. Separation of a geochemical anomaly from background by fractal andU-statistic methods, a case study: Khooni district, Central Iran. Chemie der Erde-Geochemistry, 76: 491-499.

Muller, J., Kylander, M., Martinez-Cortizas, A., Wüst, R.A, Weiss, D., Blake, K., Coles, B., Garcia-Sanchez, R., 2008. The use of principle component analyses in characterizing trace and major elemental distribution in a 55 kyr peat deposit in tropical Australia: implications to paleoclimate. Geochimica et Cosmochimica Acta, 72: 449–463.

Naimi-Ghassabian, N., Khatib, M.M., Nazari, H., Heyhat, M.R., 2016. Fractal dimension and earthquake frequency-magnitude distribution in the North of Central-East Iran Blocks (NCEIB). Geopersia, 6: 243-264.

Nazarpour, A., Rashidnejad, N., Rostami, G.H., Sadeghi, B., Matroud, F., Mehrabi, A., 2015. Application of classical statistics, log ratio transformation and multifractal approaches to delineate geochemical anomalies in the Zarshurangold district, NW, Iran. Chemie der Erde-Geochemistry, 75: 117–132.

Omrani, J., Agard, P., Whitechurch, H., Benoit, M., Prouteau, G., Jolivet, L., 2008. Arc-magmatism and subduction history beneath the Zagros Mountains, Iran: A new report of adakites and geodynamic consequences. Lithos, 106: 380–398.

Parsa, M., Maghsoudi, A., Ghezelbash, R., 2016. Decomposition of anomaly patterns of multi-element geochemical signatures in Ahar area, NW Iran: a comparison of U-spatial statistics and fractal models. Arabian Journal of Geosciences, 9: 260.

Parsa, M., Maghsoudi, A., Yousefi, M., Sadeghi, M., 2016. Recognition of significant multi-element geochemical signatures of porphyry Cu deposits in Noghdouz area, NW Iran. Journal of Geochemical Exploration, 165: 111-124.

Parsa, M., Maghsoudi, A., Yousefi, M., Sadeghi, M., 2017a. Multifractal analysis of stream sediment geochemical data: Implications for hydrothermal nickel prospection in an arid terrain, eastern Iran. Journal of Geochemical Exploration, 181: 305-317.

Parsa, M., Maghsoudi, A., Carranza, E.J.M., Yousefi, M., 2017b. Enhancement and mapping of weak multivariate stream sediment geochemical anomalies in Ahar Area, NW Iran. Natural Resources Research, 26: 443-455.

Parsa, M., Maghsoudi, A., Yousefi, M., 2018. Spatial analyses of exploration evidence data to model skarn-type copper prospectivity in the Varzaghan district, NW Iran. Ore Geology Reviews, 92: 97-112.

Radfar, J., 1999. Geologic map of the Ardestan. Geological Survey of Iran, Scale 1:100,000

Rajabpour, Sh., Abedini, A., Alipour, S., Lehmann, B., Yong Jiang, Sh., 2017. Geology and geochemistry of the sediment-hosted Cheshmeh-Konan redbed-type copper deposit, NW Iran. Ore Geology Reviews, 86: 154–171.

Reimann, C., Filzmoser, P., Garrett, R.G., 2002. Factor analysis applied to regional geochemical data: problems and possibilities. Applied Geochemistry, 17: 185–206.

Rezaei, S., Lotfi, M., Afzal, A., Jafari, M.R., Shamseddin Meigoony, M., 2015. Delineation of Cu prospects utilizing multifractal modeling and stepwise factor analysis in Noubaran 1:100,000 sheet, Center of Iran. Arabian Journal of Geosciences, 8: 7343–7357.

Rose, A., Hawkes, H., Webb, J., 1979. Geochemistry in Mineral Exploration. AcademicPress, London, 657p.

Sadeghi, B., Madani, N., Carranza, E.J.M., 2015. Combination of geostatistical simulation and fractal modeling for mineral resource classification. Journal of Geochemical Exploration, 149: 59–73.

Sadeghi, B.,Moarefvand, P., Afzal, P., Yasrebi, A.B., DaneshvarSaein, L., 2012. Application of fractal models to outline mineralized zones in the Zaghia iron ore deposit, Central Iran. Journal of Geochemical Exploration, 122: 9–19.

Shafiei, B., Haschke, M., Shahabpour, J., 2009. Recycling of orogenic arc crust triggers porphyry Cu mineralization in Kerman Cenozoic arc rocks, southeastern Iran. Mineralium Deposita, 44: 265–283.

Shahabpour, J., 2007. Island - arc affinity of the central Iranian volcanic belt. Journal of Asian Earth Sciences, 30: 652–665.

Shahabpour, J., 2005. Tectonic evolution of the orogenic belt in the region located between Kerman and Neyriz. Journal of Asian Earth Sciences, 24: 405–417.

Shahabpour, J., 1994. Post-mineral breccia dyke from the Sar-Cheshmeh porphyry copper deposit, Kerman, Iran. Exploration and Mining Geology, 3: 39–43.

Shamseddin Meigoony, M., Afzal, P., Gholinejad, M., Yasrebi, A.B., Sadeghi, B., 2013. Delineation of geochemical anomalies using factor analysis and multifractal modeling based on stream sediments data in Sarajeh 1:100,000 sheet, Central Iran. Arabian Journal of Geosciences, 7: 5333-5343.

Shelley, D., 1993. Igneous and metamorphic rocks under the microscope. Chapman and Hall, London, 630 p.

Stanley, C.R., Sinclair, A.J., 1989. Comparison of probability plots and the gap statistic in the selection of thresholds for exploration geochemistry data. Journal of Geochemical Exploration, 32: 355–357.

Stocklin, J.O., 1977. Structural correlation of the Alpine ranges between Iran and Central Asia. Memoir Hors Service Societe Geologique France, 8: 333–353.

Sun, X., Deng, J., Gong, Q., Wang, Q., Yang, L., Zhao, Z., 2009. Kohonen neural network and factor analysis based approach to geochemical data pattern recognition. Journal of Geochemical Exploration, 103: 6–16.

Treiblmaier, H., Filzmoser, P., 2010. Exploratory factor analysis revisited: how robust methods support the detection of hidden multivariate data structures in IS research. Information and management, 47: 197–207.

Tripathi, V.S., 1979. Factor analysis in geochemical exploration. Journal of Geochemical Exploration, 11: 263–275.

Wang, Q.F., Deng, J., Wan, L., Zhao, J., Gong, Q.J., Yang, L.Q., Zhou, L., Zhang, Z.J., 2008. Multifractal analysis of the element distribution in skarn-type deposits in Shizishan Orefield in Tongling area, Anhui province, China. Acta Geologica Sinica (English edition), 82: 896–905.

Wang, H., Zuo, R., 2015. A comparative study of trend surface analysis and spectrum–area multifractal model to identify geochemical anomalies. Journal of Geochemical Exploration, 155: 84-90.

Wang, Q., Deng, J., Liu, H., Wan, L., and Zhang, Z., 2011, Fractal analysis of the ore-forming process in a skarn deposit: a case study in the Shizishan area, China. Geological Society, 350: 89-104.

Yousefi, M., Kamkar-Rouhani, A., Carranza, E.J.M., 2012. Geochemical mineralization probability index (GMPI): a new approach to generate enhanced stream sediment geochemical evidential map for increasing probability of success in mineral potential mapping. Journal of Geochemical Exploration, 115: 24-35.

Yousefi, M., Kamkar-Rouhani, A., Carranza, E.J.M., 2014. Application of staged factor analysis and logistic function to create a fuzzy stream sediment geochemical evidence layer for mineral prospectivity mapping. Geochemistry Exploration Environment Analysis, 14: 45-58.

Zarasvandi, A., Rezaei, M., Sadeghi, M., Lentz, D., Adelpour, M., Pourkaseb, H., 2015. Rare earth element signatures of economic and sub-economic porphyry copper systems in Urumieh - Dokhtar magmatic arc (UDMA), Iran. Ore Geology Reviews, 70: 407-423.

Zhao, M.Y., Zhao, W.W., Liu, Y. X., 2015. Comparative analysis of soil parti- cle size distribution and its influence factors in different scales: a case study in the Loess Hilly-gully area. Acta Ecologica Sinica, 35: 4625–4632.

Ziaii, M., Pouyan, A.A., Ziaei, M., 2009. Neuro-fuzzy modeling in mining geochemistry: identification of geochemical anomalies. Journal of Geochemical Exploration, 100: 25–36.

Zuo, R., Cheng, Q., Xia, Q., 2009. Application of fractal models to characterization of vertical distribution of geochemical element concentration. Journal of Geochemical Exploration, 102: 37–43.

Zuo, R., Xia, Q., Wang, H., 2013. Compositional data analysis in the study of integrated geochemical anomalies associated with mineralization. Applied Geochemistry, 28: 202-211.